



## The underappreciated role of nonvolatile cations on aerosol ammonium-sulfate molar ratios

Hongyu Guo<sup>1</sup>, Athanasios Nenes<sup>1,2,3,4</sup>, Rodney J. Weber<sup>1</sup>

<sup>1</sup> School of Earth and Atmospheric Sciences, Georgia Institute of Technology, Atlanta, GA 30332, USA

<sup>2</sup> School of Chemical and Biomolecular Engineering, Georgia Institute of Technology, Atlanta, GA 30332, USA

<sup>3</sup> Institute for Chemical Engineering Sciences, Foundation for Research and Technology – Hellas, Patras, GR-26504, Greece

<sup>4</sup> Institute for Environmental Research and Sustainable Development, National Observatory of Athens, P. Penteli, Athens, GR-15236, Greece

10 Correspondence to: Rodney J. Weber, ([rweber@eas.gatech.edu](mailto:rweber@eas.gatech.edu)), Athanasios Nenes ([athanasios.nenes@gatech.edu](mailto:athanasios.nenes@gatech.edu))

**Abstract.** Overprediction of fine particle ammonium-sulfate molar ratios ( $R$ ) by thermodynamic models is suggested as evidence for an organic film that only inhibits the equilibration of gas phase ammonia (but not water or nitric acid) with aerosol sulfate and questions the equilibrium assumption long thought to apply for submicron aerosol. The ubiquity of such organic films implies significant impacts on aerosol chemistry. We test the organic film hypothesis by analyzing ambient observations with a thermodynamic model and find that  $R$  and ammonia partitioning can be accurately reproduced when small amounts of nonvolatile cations (NVC), consistent with observations, are considered in the thermodynamic analysis. Exclusion of NVCs results in predicted  $R$  consistently near 2. The error in  $R$  is positively correlated with NVC and not organic aerosol mass fraction or concentration. These results strongly challenge the postulated ability of organic films to perturb aerosol acidity or prevent ammonia from achieving gas-particle equilibrium for the conditions considered.

15  
20



## 1. Introduction

pH is a fundamental aerosol property that affects aerosol formation and composition through pH-sensitive reactions (Jang et al., 2002; Eddingsaas et al., 2010; Surratt et al., 2010) and gas-particle partitioning of semivolatile species (Guo et al., 2016; Guo et al., 2017a). Acidity also modulates aerosol toxicity and atmospheric nutrient supply to the oceans through changing solubility of transition metals (Meskhidze et al., 2003; Nenes et al., 2011; Longo et al., 2016; Fang et al., 2017). Despite its importance, the inability to directly measure fine mode particle pH (e.g. Rindelaub et al. (2016) presents an indirect method that infers particle  $H^+$  activity for sizes above  $10\ \mu m$  and requires activity coefficient predicted by a thermodynamic modeling. This method reports the pH for a  $HSO_4^-/SO_4^{2-}$  aerosol system similar to the fine particle pH predicted by a thermodynamic modeling used in this study (Guo et al., 2015)) has led to the use of measurable aerosol properties as acidity proxies, such as aerosol ammonium-sulfate ratio or ion balances (e.g. (Paulot and Jacob, 2014; Wang et al., 2016; Silvern et al., 2017)). Recent work has shown that acidity proxies are not uniquely related to pH, which in turn strongly questions any conclusions derived from its use. There are numerous reasons why acidity proxies do not represent pH well; they do not capture the variability in particle water content, ion activity coefficients, or partial dissociation of species in the aerosol phase (Guo et al., 2015; Hennigan et al., 2015; Guo et al., 2016). The method that best constrains aerosol pH is comparison between a thermodynamic analysis and observations of gas-particle partitioning of semivolatile species that are sensitive to pH at the given environmental conditions (i.e., gas-particle concentration ratios near 1:1) (Guo et al., 2015; Guo et al., 2016; Weber et al., 2016; Guo et al., 2017a).  $NH_3-NH_4^+$ ,  $HNO_3-NO_3^-$ , and  $HCl-Cl^-$  pairs often meet this condition. The method has been utilized for a range of meteorological conditions (RH, T) and gas/aerosol concentrations demonstrating that model predictions are often in agreement with observations.

It has been noted that thermodynamic models fail to accurately predict ammonium-sulfate molar ratios when just considering the  $NH_4^+-SO_4^{2-}-NO_3^-$  aerosol system in equilibrium with the corresponding gas species (Kim et al., 2015; Silvern et al., 2017). In the southeastern US, where total ammonium ( $NH_x = NH_3 + NH_4^+$ ) is observed to be in large excess of particle sulfate and observed  $NH_4^+/SO_4^{2-}$  molar ratios are in the range of 1-2 (Hidy et al., 2014; Guo et al., 2015; Kim et al., 2015), thermodynamic models often predict very low pH (0.5 to 2) (Guo et al., 2015) and molar ratios close to 2 (Kim et al., 2015; Weber et al., 2016; Silvern et al., 2017). The molar ratio discrepancy has led to the hypothesis that thermodynamic predictions are incorrect, and particles are coated by organic films that inhibit the condensation of  $NH_3$  from the gas phase and give rise to the molar ratio discrepancy (Silvern et al., 2017). Such kinetic limitations, if prevalent, opposes the validity of aerosol thermodynamic equilibrium and could significantly impact aerosol chemistry and acidity-mediated processes, given the large organic aerosol mass fractions worldwide (Zhang et al., 2007) and expected increasing organic mass fractions in the future due to changing emission, such as  $SO_2$  emission reduction in the eastern US (Hand et al., 2012; Attwood et al., 2014; Hidy et al., 2014). The hypothesis of organic films, however, is in stark contrast to established literature showing that  $NH_3$ , water vapor, and  $HNO_3$  equilibrate with organic-rich aerosols (Fountoukis et al., 2009; Guo et al., 2015; Guo et al., 2016; Guo et al., 2017a). Such a film, as proposed by Silvern et al. (2017), selectively limits  $NH_3$ , but not  $H_2O$  and  $HNO_3$  molecules that are both larger than  $NH_3$  hence more difficult to diffuse through media. At low temperature or low relative humidity, aerosols may be in semi-liquid or glassy state and have very low diffusivity of molecules throughout its volume (Tong et al., 2011; Bones et al., 2012). This may severely limit gas-particle mass transfer of all components and require much longer time scales to equilibrate. However, we have not observed such an effect for the conditions in the eastern US, as there is good agreement between observed and predicted particle water, and partitioning of  $NH_3-NH_4^+$  and  $HNO_3-NO_3^-$  (the bias in  $NO_3^-$  prediction becomes progressively worse when RH drops below 40%, likely owing to glassy states during the wintertime) (Guo et al., 2015; Guo et al., 2016).

Other reasons that are unrelated to organic films may drive the molar ratio discrepancy. One is related to the variation of aerosol composition with size, which may translate to a large range of acidity, hence equilibrium composition (Keene et al., 1998; Nenes



et al., 2011; Bougiatioti et al., 2016; Fang et al., 2017). Another related issue is the presence of soluble nonvolatile cations (NVC, such as  $\text{Na}^+$ ,  $\text{K}^+$ ,  $\text{Ca}^{2+}$ ,  $\text{Mg}^{2+}$ ), which are often neglected in thermodynamic calculations because of their relatively minor contribution to aerosol mass or are not routinely included in aerosol composition measurements (e.g., those made with an aerosol mass spectrometer). Here we show that ignoring even small amounts of NVC as inputs to the thermodynamic model results in  
5 predicted  $\text{NH}_4^+/\text{SO}_4^{2-}$  molar ratios close to 2 due to the model criteria of electrical neutrality, whereas including small levels of NVC brings model-predicted molar ratios into agreement with observed levels.

## 2. Methods

**Molar ratios definition:** Two ammonium-sulfate aerosol molar ratios are used in the following analysis,

$$R = \frac{\text{NH}_4^+}{\text{SO}_4^{2-}} \quad (1)$$

$$R_{\text{SO}_4} = \frac{\text{NH}_4^+ - \text{NO}_3^-}{\text{SO}_4^{2-}} \quad (2)$$

both are based on inorganic mole concentrations in units of  $\mu\text{mol m}^{-3}$ .  $R_{\text{SO}_4}$  is a more narrowly defined molar ratio that excludes  
10  $\text{NH}_4^+$  associated with  $\text{NO}_3^-$ , because ammonium sulfate and ammonium nitrate are typically associated with different sized particles (externally mixed) (Zhuang et al., 1999) and molar ratios are calculated based on bulk composition data ( $\text{PM}_{2.5}$  or  $\text{PM}_1$ ). The upper limit for  $R$  and  $R_{\text{SO}_4}$  is 2 for a particle composition of pure  $(\text{NH}_4)_2\text{SO}_4$ , the lower limit is 0 for  $R$  when  $\text{SO}_4^{2-}$  is associated with other cations instead of  $\text{NH}_4^+$  (e.g.  $\text{Na}_2\text{SO}_4$ ) or if there is free  $\text{H}_2\text{SO}_4$  in the aerosol. A negative  $R_{\text{SO}_4}$  can occur for conditions of high  $\text{NO}_3^-$  and low  $\text{NH}_4^+$ ,  $\text{SO}_4^{2-}$  concentrations (e.g.,  $\text{NaNO}_3$ ), but rare for ambient fine particles.  $R$  or  $R_{\text{SO}_4}$  is  
15 typically observed in the range of 1 and 2 in the southeastern US (i.e., between  $\text{NH}_4\text{HSO}_4$  and  $(\text{NH}_4)_2\text{SO}_4$ ) (Hidy et al., 2014; Guo et al., 2015; Weber et al., 2016). In cases where  $\text{NO}_3^-$  levels are low relative to  $\text{SO}_4^{2-}$ , the two ratios,  $R_{\text{SO}_4}$  and  $R$ , are equivalent, as is observed in the summertime southeastern US, where  $\text{NO}_3^-$  is typically  $\sim 0.2 \mu\text{g m}^{-3}$ ,  $\text{NH}_4^+ \sim 1 \mu\text{g m}^{-3}$ , and  $\text{SO}_4^{2-} \sim 3 \mu\text{g m}^{-3}$  (Blanchard et al., 2013).

**Observations:** Two datasets are used for analysis, the Southern Oxidant and Aerosol Study (SOAS) and the Wintertime  
20 Investigation of Transport, Emissions, and Reactivity (WINTER). The SOAS study was conducted from 1 June to 15 July in the summer of 2013 at a rural ground site in Centreville (CTR), AL, representative of the southeastern US background atmosphere in summer. The WINTER data was produced from 13 research aircraft flights from 1 Feb to 15 Mar in 2015 mainly sampling over the northeastern US. Details of the campaigns and instruments, and calculations and verification of pH based on the observation datasets, have been described in Guo et al. (2015) and Guo et al. (2016), respectively. In the following analysis, we use  $R$  for  
25 summertime datasets with low  $\text{NO}_3^-$  and  $R_{\text{SO}_4}$  for wintertime datasets with high  $\text{NO}_3^-$  concentration. Both datasets report highly acidic aerosols with average  $\text{pH} \sim 1$  (Guo et al., 2015; Guo et al., 2016). At these pH levels, aerosol sulfate can be in the partially deprotonated form of  $\text{HSO}_4^-$  instead of  $\text{SO}_4^{2-}$ . For example, 14% sulfate is predicted to be  $\text{HSO}_4^-$  and the rest as  $\text{SO}_4^{2-}$  in the winter dataset (Guo et al., 2016). Free form  $\text{H}_2\text{SO}_4$ , which requires even lower pH, is rare in the ambient aerosol. The  $\text{SO}_4^{2-}$  in this study refers to the sum of total aqueous aerosol sulfate ( $\text{SO}_4^{2-}$ ,  $\text{HSO}_4^-$ , and  $\text{H}_2\text{SO}_4$ ), the same definition (i.e., S(VI)) used in  
30 Silvern et al. (2017), since aerosol instruments normally report total aqueous sulfate as just  $\text{SO}_4^{2-}$ . The same applies to  $\text{NH}_4^+$  and  $\text{NO}_3^-$ . The observation data are from two widely deployed aerosol instruments; a Particle-Into-Liquid-Sampler coupled with an Ion Chromatograph (PILS-IC) and a High-Resolution Time-of-Flight Aerosol Mass Spectrometer (hereafter referred to as AMS). The PILS-IC detects aerosol water-soluble anions and cations collected and diluted by deionized water to the extent of complete deprotonation of  $\text{H}_2\text{SO}_4$  in the aqueous sample (Orsini et al., 2003). The AMS vaporizes aerosols and ionizes non-refractory



species with a 70 eV electron impact ionization and cannot distinguish the dissociation states of inorganic ions (DeCarlo et al., 2006).

**Thermodynamic analysis of observations:** The thermodynamic model ISORROPIA-II (Fountoukis and Nenes, 2007) was used to determine the composition and phase state of an  $\text{NH}_4^+$ - $\text{SO}_4^{2-}$ - $\text{NO}_3^-$ - $\text{Cl}^-$ - $\text{Na}^+$ - $\text{Ca}^{2+}$ - $\text{K}^+$ - $\text{Mg}^{2+}$ -water inorganic aerosol (or a subset thereof) and its partitioning with corresponding gases. Using this model, we have developed a method for pH prediction that includes appropriate validation and uncertainty assessment (Guo et al., 2015) and applied the methods to several other locations (Bougiatioti et al., 2016; Guo et al., 2016; Weber et al., 2016; Guo et al., 2017a; Guo et al., 2017b). Here pH is defined following the same approach,

$$\text{pH} = -\log_{10} \gamma_{\text{H}^+} H_{\text{aq}}^+ = -\log_{10} \frac{1000 \gamma_{\text{H}^+} H_{\text{air}}^+}{W_i + W_o} \cong -\log_{10} \frac{1000 \gamma_{\text{H}^+} H_{\text{air}}^+}{W_i} \quad (3)$$

where  $\gamma_{\text{H}^+}$  is the hydronium ion activity coefficient (assumed = 1),  $H_{\text{aq}}^+$  ( $\text{mol L}^{-1}$ ) the hydronium ion concentration in particle liquid water,  $H_{\text{air}}^+$  ( $\mu\text{g m}^{-3}$ ) the hydronium ion concentration per volume of air, and  $W_i$ ,  $W_o$  ( $\mu\text{g m}^{-3}$ ) are particle water concentrations associated with inorganic and organic species, respectively. pH predicted solely with  $W_i$  is fairly accurate; pH was 0.15-0.23 units systematically lower than and highly correlated to ( $r^2 = 0.97$ ) pH predicted with total particle water ( $W_i + W_o$ ) in the southeast, where  $W_o$  accounted for 35% of total particle water (Guo et al., 2015). For simplicity, we therefore use  $W_i$  for the following pH calculations.

ISORROPIA-II was run in “forward” mode to calculate gas-particle equilibrium concentrations based on the input of total concentration of various inorganic species (e.g.,  $\text{NH}_3 + \text{NH}_4^+$ ). The best agreement between model and observations were achieved assuming “metastable” particles with no solid precipitates ( $\text{H}^+$  is not stable in an effloresced aerosol). We also assumed that the particles were internally mixed, and that pH did not vary with size (so that bulk properties represent the aerosols, including pH) and gas-particle partitioning was in thermodynamic equilibrium. For submicron aerosol ( $\text{PM}_{10}$ ), equilibrium states are typically achieved within 30 minutes under ambient conditions (Dassios and Pandis, 1999; Cruz et al., 2000; Fountoukis et al., 2009). The prediction of gas-particle partitioning has been found to be in good agreement with observations when using particle bulk concentrations as model input (Guo et al., 2015; Guo et al., 2016; Guo et al., 2017a), although particle pH is size dependent. pH increases for particles above  $1 \mu\text{m}$  as a result of NVC (Fang et al., 2017) resulting in particle mixing state becoming more important with increasing particle size (Guo et al., 2017a). ISORROPIA input data files for the analyses reported in this paper are provided with the supplementary material.

### 3. Discussion

**The cause for discrepancy between modeled and measured molar ratios (R):** We first investigate the issue of  $R$  discrepancy using PILS-IC  $\text{PM}_{2.5}$  data from a 12-day period (11-23 June) of the SOAS campaign. The same period has been used to study pH sensitivity to sulfate and ammonia and shown to accurately predict  $\text{NH}_3$ - $\text{NH}_4^+$  partitioning compared to observations (Weber et al., 2016). To test the sensitivity of ISORROPIA-II predictions, we ran the model with the same input as Weber et al. (2016), (inputs include  $\text{Na}^+$ , ( $\text{NH}_4^+ + \text{NH}_3$ ),  $\text{SO}_4^{2-}$ ,  $\text{NO}_3^-$ ,  $\text{Cl}^-$ ,  $\text{Ca}^{2+}$ ,  $\text{Mg}^{2+}$ ,  $\text{K}^+$ , RH, T, where  $\text{Ca}^{2+}$ ,  $\text{Mg}^{2+}$ ,  $\text{K}^+$  inputs were zero,  $\text{NH}_4^+$ ,  $\text{SO}_4^{2-}$ ,  $\text{NO}_3^-$ ,  $\text{Cl}^-$  concentrations were from PILS-IC  $\text{PM}_{2.5}$  observational data,  $\text{NH}_3$  was from chemical ionization mass spectrometer measurements (You et al., 2014)) and tested three different  $\text{Na}^+$  levels: (1)  $\text{Na}^+$  determined from an ion charge balance by  $\text{Na}^+ = 2\text{SO}_4^{2-} + \text{NO}_3^- + \text{Cl}^- - \text{NH}_4^+$  (unit:  $\mu\text{mol m}^{-3}$ ); (2) measured  $\text{PM}_{2.5}$   $\text{Na}^+$  from PILS-IC; (3)  $\text{Na}^+ = 0$ . Different  $\text{Na}^+$  concentrations were used to investigate the impact of  $\text{Na}^+$  on model output. The inferred  $\text{Na}^+$  was on average  $0.28 \pm 0.18 \mu\text{g m}^{-3}$ , higher than the measured level of  $0.06 \pm 0.09 \mu\text{g m}^{-3}$ . Note that, the limit of detection (LOD) of PILS-IC  $\text{Na}^+$  in



this study was  $0.07 \mu\text{g m}^{-3}$ , close to the reported average level. Unlike the standard procedure of reporting below LOD values as  $\frac{1}{2}$  LOD, we use the  $\text{Na}^+$  concentrations directly from the instrument, including those below the LOD because, as will be shown,  $R$  is highly sensitive to trace levels of NVC. Also, we note that all other NVC, such as  $\text{Ca}^{2+}$  and  $\text{Mg}^{2+}$ , were generally below the PILS-IC LOD (therefore set to zero in the model input). The charge balance predicted  $\text{Na}^+$  should then be viewed, for this data set, as the concentration of generic NVC concentrations with a valence of 1. The charge balance predicted  $\text{Na}^+$  must be above zero; for calculated values below zero (8 out of 229 points, 3% of the data), due to combined measurement uncertainty, a small positive value of  $0.005 \mu\text{g m}^{-3}$  is assigned.

The concentration of  $\text{H}^+$  is also ignored in the ion charge balance calculation as it is 2-3 orders of magnitude smaller than the major inorganic ions, even at these low pH (between 0 and 2). For example, the average  $\text{PM}_{2.5}$  mole concentrations per volume of air for the ions measured by the PILS-IC were  $\text{NH}_4^+ = 0.0354$ ,  $\text{SO}_4^{2-} = 0.0211$ ,  $\text{NO}_3^- = 0.0037$ ,  $\text{Na}^+ = 0.0029$ , and  $\text{Cl}^- = 0.00082 \mu\text{mol m}^{-3}$ , compared to ISORROPIA-predicted  $\text{H}^+ = 0.00031 \mu\text{mol m}^{-3}$  for this period. The observed  $\text{Na}^+$  appeared to be mainly associated with  $\text{NO}_3^-$ , and to a lesser degree with  $\text{Cl}^-$ , based on high linear correlations,  $r^2 = 0.82$  and  $0.64$ , respectively. A typical level of “chloride depletion” was observed as a  $\text{Cl}^-/\text{Na}^+$  ratio of  $0.24 \pm 0.16$  ( $\text{mol mol}^{-1}$ ), due to higher volatility of  $\text{HCl}$  versus  $\text{HNO}_3$  (Fountoukis and Nenes, 2007). In this case,  $\text{Cl}^-$  input to ISORROPIA is negligible as it does not affect the predictions of pH or molar ratios due to the measured  $\text{Cl}^-$  concentration being small,  $0.03 \pm 0.04 \mu\text{g m}^{-3}$  ( $\text{LOD} = 0.01 \mu\text{g m}^{-3}$ ). Fig. 1 shows the time series of various parameters for the SOAS 12-day period investigated. From these data, the effect of  $\text{Na}^+$  (i.e., NVC) on ISORROPIA-predicted  $\text{SO}_4^{2-}$ ,  $\text{NH}_4^+$ ,  $\text{NH}_3$ ,  $R$ , and pH is investigated. Fig. 1a and Fig. 1d show the overall behavior of total ammonium ( $\text{NH}_x = \text{NH}_3 + \text{NH}_4^+$ ) and sulfate.  $\text{SO}_4^{2-}$  is nonvolatile so remains unchanged by the model, as does total ammonium and hence the  $\text{NH}_x/\text{SO}_4^{2-}$  molar ratio. Therefore, the discrepancy between modeled and measured  $R$  must result from the  $\text{NH}_4^+$  prediction. It is noteworthy that  $\text{NH}_x/\text{SO}_4^{2-}$  is generally above 2, indicating excess  $\text{NH}_x$  compared to  $\text{SO}_4^{2-}$ . Under such conditions, it is often interpreted that  $\text{NH}_3$  must completely neutralize  $\text{SO}_4^{2-}$  (Kim et al., 2015; Silvern et al., 2017). The thermodynamic model predicts otherwise; despite the excess  $\text{NH}_x$ ,  $\text{PM}_{2.5}$  is predicted to be highly acidic, with a pH range between 0 and 2 (Fig. 1h), resulting from  $\text{NH}_4^+$  semivolatility and  $\text{SO}_4^{2-}$  being virtually nonvolatile at any atmospherically-relevant concentration and acidity (Weber et al., 2016).

The predicted time series of  $\text{NH}_3$ - $\text{NH}_4^+$  partitioning agrees most with observations when measured  $\text{Na}^+$  (Fig. 2) is included in the model compared to model results with identical inputs, except with zero  $\text{Na}^+$  or inferred  $\text{Na}^+$  from ion charge balance (Fig. 1e, 1f, 1g, and Fig. 2). For ISORROPIA simulations with measured  $\text{Na}^+$  as input, the orthogonal linear regression of ISORROPIA-predicted versus measured particle phase fractions of total ammonium, where  $\epsilon(\text{NH}_4^+) = \text{NH}_4^+/\text{NH}_x$ , is:  $\epsilon(\text{NH}_4^+)_{\text{predicted}} = (1.00 \pm 0.03) \epsilon(\text{NH}_4^+)_{\text{observed}} + (0.03 \pm 0.02)$ , with  $r^2 = 0.76$  and “ $\pm$ ” is one standard deviation (SD). Mean  $\epsilon(\text{NH}_4^+)_{\text{observed}}$  was  $54 \pm 13\%$ , making the partitioning sensitive to pH (Guo et al., 2017a). As the nonvolatile  $\text{Na}^+$  competes with semivolatile  $\text{NH}_4^+$ , predicted  $\text{NH}_4^+$  decreases when higher levels of  $\text{Na}^+$  are input to the model, whereas predicted gas phase  $\text{NH}_3$  increases for conservation of input  $\text{NH}_x$ . Thus, since the ion charge balance inferred  $\text{Na}^+$  is often higher than measured  $\text{Na}^+$  (Fig. 1c), the lowest  $\text{NH}_4^+$  and  $\epsilon(\text{NH}_4^+)$  are predicted with the input of inferred  $\text{Na}^+$ . In contrast, the highest  $\text{NH}_4^+$  and  $\epsilon(\text{NH}_4^+)$  are predicted with zero  $\text{Na}^+$  input, whereas the predicted values with measured  $\text{Na}^+$  as model input are between these two. For the period in Fig. 1, measured  $\text{Na}^+$  was  $0.06 \mu\text{g m}^{-3}$  and the inferred value was  $0.28 \mu\text{g m}^{-3}$ .

$R$  also depends on the input  $\text{Na}^+$  concentration. For the Fig. 1 period, predicted  $R$  was on average  $1.43 \pm 0.32$  for an ISORROPIA input with inferred  $\text{Na}^+$ ,  $1.85 \pm 0.17$  for measured  $\text{Na}^+$  input, and the highest  $R$  at  $1.97 \pm 0.02$  when zero  $\text{Na}^+$  was used as model input. The average measured  $R$  was  $1.70 \pm 0.23$  by PILS-IC and  $1.75 \pm 0.20$  by another  $\text{PM}_{2.5}$  water-soluble ion measurement (Allen et al., 2015). Thus, model  $R$  with measure  $\text{Na}^+$  input was closest to the measured  $R$ . Under the meteorological conditions of the southeast in summertime ( $T = 25 \pm 5 \text{ }^\circ\text{C}$ ,  $\text{RH} = 68 \pm 18 \%$ ), the thermodynamic model predicts  $R$  always near or equal to



2, when input NVCs are set to zero and the only other particle composition inputs are  $\text{SO}_4^{2-}$ ,  $\text{NH}_4^+$ , and  $\text{NO}_3^-$ , with paired gases  $\text{NH}_3$  or  $\text{HNO}_3$ , indicating a particle composition of mainly  $(\text{NH}_4)_2\text{SO}_4$ ; expected for electroneutrality of the aerosol aqueous phase. These are the model inputs when particle composition are from an AMS (e.g. (Kim et al., 2015; Silvern et al., 2017)) and explains why ISORROPIA-predicted  $R$  disagreed with measured values, which is a basis for the organic film hypothesis (Silvern et al., 2017).

Contrasts between measured and predicted  $R$  for periods of differing model input  $\text{Na}^+$  levels can be seen in Fig. 1. First, if the ambient  $\text{Na}^+$  mass concentration was higher than the PILS-IC LOD, such as the period of 11-13 & 16 June, the predicted and measured  $R$  agree when measured  $\text{Na}^+$  is input. Inferred  $\text{Na}^+$  from the ion charge balance appears to be overestimated at these times, and this causes a noticeable bias in the prediction of  $R$ ,  $\text{NH}_3$ ,  $\text{NH}_4^+$ , and  $\epsilon(\text{NH}_4^+)$ . The pH calculated based on the inferred  $\text{Na}^+$  also differs compared to the pH calculated from the measured  $\text{Na}^+$  for this period. During periods when ambient  $\text{Na}^+$  mass concentration was below the measurement LOD but close to zero, no discrepancy in  $R$  is found since both values are near 2 (e.g., around the time of 16 June midnight). This results from negligible effects of NVC since concentrations are very low. When ambient  $\text{Na}^+$  concentrations were below LOD but not zero, there is a discrepancy between predicted and observed  $R$  for ISORROPIA with input of measured  $\text{Na}^+$  or zero  $\text{Na}^+$ , however, inferred  $\text{Na}^+$  results in better agreement. For instance, during the period of 18-20 & 22-23 June, the predicted  $R$  with the inferred  $\text{Na}^+$  input follows (but is slightly lower than) observations; this is consistent with an overestimation of  $\text{Na}^+$  from the ion charge balance calculation. Overall, the time series analysis demonstrates how model-predicted molar ratios are affected by measurement accuracy and LODs of NVC and the sensitivity of ISORROPIA-predicted  $R$  to NVCs input concentrations. Note that a few measured  $R$  points were above 2 (e.g. midnight of 15 June), a result of measurement uncertainty and error propagation at low  $\text{SO}_4^{2-}$  concentrations.

**20 Quantification of NVC effects on  $R$  and pH:** We have shown that the discrepancy in  $R$  can be resolved for this data set by adding small amounts of  $\text{Na}^+$ , either measured (when near or above LOD) or inferred from an ion charge balance analysis when not measured or significantly below the measurement method LOD. However, due to propagation of  $\text{SO}_4^{2-}$ ,  $\text{NH}_4^+$ , and  $\text{NO}_3^-$  measurement errors, the uncertainty in inferred  $\text{Na}^+$  data may cause a noticeable bias in the prediction of  $R$  or pH, such as observed on 11-13 June (Fig. 1b). Because of this, quantifying the sensitivities of  $R$  and pH to  $\text{Na}^+$ , or any other NVC, is of interest. Here we use  $\text{Na}^+$  as an example since it was the highest NVC concentration measured in this study;  $\text{K}^+$  and  $\text{Mg}^{2+}$  have similar effects.  $\text{Ca}^{2+}$  behaves differently due to  $\text{CaSO}_4$  solids precipitating out, shown as Fig. S1 in the supplement.

Differences in predicted  $R$  with and without measured  $\text{Na}^+$  are plotted against  $\text{Na}^+$  mass and organic aerosol mass fractions in Fig. 3a;  $\Delta R$  is defined as ISORROPIA predicted  $R$  with  $\text{Na}^+$  minus ISORROPIA predicted  $R$  without  $\text{Na}^+$ . Fig. 3a shows that  $\Delta R$  is highly correlated with  $\text{Na}^+$  ( $r^2 = 0.93$ ). Based on an orthogonal linear regression  $\Delta R = (-1.74 \pm 0.03) \text{Na}^+ + (0.001 \pm 0.003)$ . From the regression slope, the average measured  $\text{Na}^+$  level of  $0.06 \mu\text{g m}^{-3}$ , a background level of  $\text{PM}_{2.5} \text{Na}^+$  in the southeast, causes a response of  $-0.10$  in  $R$ . At a  $\text{Na}^+$  level of only  $0.3 \mu\text{g m}^{-3}$ ,  $\Delta R$  reaches  $-0.5$ , indicating a rapid decrease from  $R = 2$  (no NVC) to  $R = 1.5$  (with NVC) for these conditions. Thus, not only is  $\Delta R$  highly correlated with  $\text{Na}^+$ , it is also highly sensitive to  $\text{Na}^+$ . This is not seen for the organic aerosol mass fraction, here used as a proxy for the thickness of a possible film because it constrains the organic volume per particle. (A similar plot based on organic aerosol mass concentration is shown in Fig. S2). In stark contrast to  $\text{Na}^+$ , Fig. 3a shows no correlation between  $\Delta R$  and organic aerosol mass fraction. (There is also no correlation when  $\Delta R$  is plotted against OA mass concentration for data points  $\Delta R = \text{measured } R - 2$ , and an inverse correlation is observed for some points between  $\Delta R$  and organic aerosol mass concentration for  $\Delta R = \text{predicted } R \text{ (with } \text{Na}^+) - \text{predicted } R \text{ (no } \text{Na}^+)$ , see Fig. S2 in the supplement). These results are inconsistent with the bias in  $R$  being linked to increases in mass fraction of organic species, as proposed by Silvern et al. (2017).





In comparison to  $R$ , pH is less sensitive to inclusion of  $\text{Na}^+$ , or other NVCs in general.  $\Delta\text{pH}$  is only 0.07 for the average  $\text{Na}^+$  level of  $0.06 \mu\text{g m}^{-3}$ , and increases to 0.38 at  $0.3 \mu\text{g m}^{-3} \text{Na}^+$  (Fig. 3b). The magnitude of  $\Delta\text{pH}$  is relatively small and consistent with our previous studies where we investigated the effects of sea-salt on pH (Guo et al., 2016; Weber et al., 2016).  $\Delta\text{pH}$  would be higher in regions with more abundant NVC. For instance, a  $\Delta\text{pH}$  of 0.8 unit was found in Pasadena, CA, where the average  $\text{PM}_{2.5}$   $\text{Na}^+$  mass was  $0.77 \mu\text{g m}^{-3}$  (Guo et al., 2017a). Differences in sensitivity of  $R$  and pH to  $\text{Na}^+$  can be seen based on linear regressions. The magnitude of the  $\Delta R\text{-Na}^+$  slope is  $-1.74$  compared to  $\Delta\text{pH-Na}^+$  slope of 1.27. Sensitivities of pH and  $R$  (or  $R_{\text{SO}_4}$ ) to  $\text{Na}^+$  are discussed further below, next we investigate NVC effects on  $R$  and pH for a different data set.

**NVC Effects on molar ratios and pH based on winter data:** The above discussion is based on data collected at a ground site in summertime (SOAS), we expand the investigation of the  $R$  discrepancy to a larger geographical scale and for a different season by performing a similar analysis with the WINTER study data set collected in wintertime. In this study, NVCs were generally higher, especially when the aircraft sampled near coastlines (e.g.  $\text{PM}_1 \text{Na}^+ = 0.23 \mu\text{g m}^{-3}$ ). Also,  $\text{PM}_1$  nitrate was comparable to sulfate, largely owing to lower temperatures ( $\text{NO}_3^- 0.013 \mu\text{mol m}^{-3}$  vs.  $\text{SO}_4^{2-} 0.011 \mu\text{mol m}^{-3}$ ) (Guo et al., 2016). Therefore,  $R_{\text{SO}_4}$  was calculated instead of  $R$ . In this case the aerosol inorganic composition data input for ISORROPIA-II is from an AMS. Since the AMS does not efficiently detect ions associated with refractory species, such as  $\text{Na}^+$  and associated  $\text{Cl}^-$  from  $\text{NaCl}$ , in our past analysis of the WINTER aerosol pH, we only included  $\text{NH}_4^+$ ,  $\text{SO}_4^{2-}$ , and total nitrate ( $\text{NO}_3^- + \text{HNO}_3$ ) as input for ISORROPIA-II. ( $\text{NH}_3$  should be included, but was not measured, although in this case it was found to have a small effect on predicted pH:  $\sim 0.2$  higher pH when including an  $\text{NH}_3$  concentration of  $0.10 \mu\text{g m}^{-3}$  determined from an iteration method). With these assumptions, we found good agreement between predicted and measured  $\text{HNO}_3\text{-NO}_3^-$  partitioning (average  $\epsilon(\text{NO}_3^-) = 39\%$ ), especially when RH was above 60% (Guo et al., 2016). However, again Fig. 4a shows that the model overpredicted  $R_{\text{SO}_4}$ . Also, when concentrations of NVC were low, predicted and measured  $R_{\text{SO}_4}$  was generally 2. (Note that the predicted  $R_{\text{SO}_4}$  should be biased low since  $\text{NH}_4^+$  was underpredicted due to lack of  $\text{NH}_3$  data, resulting in some fraction of input particle phase  $\text{NH}_4^+$  repartitioned in the model to the gas phase). On average, predicted  $R_{\text{SO}_4}$  was  $1.68 \pm 0.51$  versus the measured value of  $1.47 \pm 0.43$ . In Fig 4a, the gray error bars show the propagated uncertainties for  $R_{\text{SO}_4}$  based on a 35% AMS measurement uncertainty for  $\text{NH}_4^+$ ,  $\text{SO}_4^{2-}$ , and  $\text{NO}_3^-$  (Bahreini et al., 2009).

As in the SOAS data set, including NVCs also brings predicted and measured ammonium-sulfate molar ratios into agreement (Fig. 4b). Here, the amounts of NVC needed for an ion charge balance involving  $\text{NVC-NH}_4^+\text{-SO}_4^{2-}\text{-NO}_3^-$  aerosols were calculated based solely on NVC assumed to be  $\text{Na}^+$  (the thermodynamic results based on other NVCs are shown in the supplemental material in Fig. S3.  $\text{K}^+$  and  $\text{Mg}^{2+}$  work similarly to  $\text{Na}^+$ , while  $\text{Ca}^{2+}$  can precipitate sulfate in the form of  $\text{CaSO}_4$ ). Overall,  $\text{Na}^+$  is chosen as a proxy NVC in our dataset because it constitutes most of the NVC mass and does not precipitate out of solution. The choice of  $\text{Na}^+$  as a NVC proxy, although appropriate here, is not generally applicable; in regions with considerable dust contributions, treating NVC as “equivalent  $\text{Na}^+$ ” in the thermodynamic calculations can result in large prediction errors (e.g., (Fountoukis et al., 2009)). As done before, in this analysis, when the ion charge balance predicts negative  $\text{Na}^+$  concentrations (137 data points out of 3226, 4%), a small positive value of  $0.005 \mu\text{g m}^{-3}$  is assigned. It is clear in Fig. 4b that with the added NVC, the predicted  $R_{\text{SO}_4}$  is in good agreement with the observation, with regression result  $R_{\text{SO}_4,\text{predicted}} = (1.05 \pm 0.01) R_{\text{SO}_4,\text{observed}} + (-0.12 \pm 0.01)$ ,  $r^2 = 0.99$ . Again, the molar ratio bias from the thermodynamic model is simply a matter of not including small amounts of NVC (e.g.  $0.15 \mu\text{g m}^{-3} \text{Na}^+$  or  $0.26 \mu\text{g m}^{-3} \text{K}^+$ ). The average amount of inferred  $\text{Na}^+$  from the ion charge balance in this case is smaller than what was measured offline during the study;  $\text{PM}_1 \text{Na}^+$  of  $0.23 \mu\text{g m}^{-3}$  (Guo et al., 2016). The analysis using measured  $\text{PM}_1 \text{Na}^+$  results in highly scattered data due to the high sensitivities of  $R_{\text{SO}_4}$  to NVC and the significant  $\text{Na}^+$  measurement uncertainty at these low levels and the analytical method used in this study.



- Because molar ratios are sensitive to NVCs and NVC concentrations are often very low, use of molar ratios to test the thermodynamic model should be done with caution, but actually not recommended. Since NVC associated with sea-salt and crustal materials are normally very small fractions of the PM<sub>1</sub> inorganic mass, it is typically reasonable to ignore these species when determining PM<sub>1</sub> NH<sub>4</sub><sup>+</sup> and NO<sub>3</sub><sup>-</sup> partitioning, or pH, using ISORROPIA-II, as we have shown (Guo et al., 2016; Guo et al., 2017a). Since the molar ratio is a pH proxy that is highly sensitive to small mass concentrations of NVCs, as well as measurement errors, and only provides limited insights on pH and its effects (see discussion in the Introduction), we view this as a minor issue since pH should be used instead (Guo et al., 2017a). Alternatively, if accurate NVC data is not available, NVC can be estimated through an ion charge balance calculation with the measured NH<sub>4</sub><sup>+</sup>-SO<sub>4</sub><sup>2-</sup>-NO<sub>3</sub><sup>-</sup> data and include the resulting inferred NVC in the ISORROPIA input, which will produce a better estimate of *R* than setting NVC to zero in the model input.
- 5 **Effects of not fully considering NVC of pH:** The molar ratios and pH reported for SOAS (Guo et al., 2015) and WINTER (Guo et al., 2016) may exhibit biases since NVCs were not fully considered. This was because the NVC (Na<sup>+</sup>, K<sup>+</sup>, Ca<sup>2+</sup>, Mg<sup>2+</sup>) concentrations were low, often close to or below the PILS-IC LOD during the SOAS study (the 1<sup>st</sup> half period measuring PM<sub>2.5</sub> and the 2<sup>nd</sup> half period measuring PM<sub>1</sub> with even lower NVC) and not measured by an AMS during the WINTER study. We have discussed the effect of NVC on *R* and *R*<sub>SO4</sub> above, here we focus on the effect on pH and the implications.
- 15 In our datasets, ion charge balance inferred Na<sup>+</sup> (or K<sup>+</sup>, Mg<sup>2+</sup>) is an upper limit (for assuming complete dissociation; e.g., all sulfate is in the form of SO<sub>4</sub><sup>2-</sup>) on soluble NVC based on the observed NH<sub>4</sub><sup>+</sup>-SO<sub>4</sub><sup>2-</sup>-NO<sub>3</sub><sup>-</sup> data, and satisfies the criterion of aerosol electrical neutrality. As shown above, H<sup>+</sup> is negligible in ion charge balance calculation even at such low pH of 1. Using an inferred Na<sup>+</sup> as a reference value, a worst case of zero NVC in the input results in an underestimation of pH by 0.32 for SOAS and 0.49 for WINTER, and overestimation of molar ratios by 0.58 for SOAS (*R*) and 0.62 for WINTER (*R*<sub>SO4</sub>), respectively.
- 20 Using measured Na<sup>+</sup> as input instead of zero NVC results in a difference in pH of -0.26 and 0.22, and in molar ratio of 0.46 (*R*) and -0.33 (*R*<sub>SO4</sub>), for SOAS and WINTER, respectively. (See Section 4 in the supplemental material). NVCs are seen to have a larger effect on molar ratios than pH based on the regression slopes (see Fig. 3), and the effect is even more pronounced considering observed ranges in molar ratios (*R* or *R*<sub>SO4</sub> from 0 to 2) are less than pH (from -1 to 3) (see Fig. S5) (Guo et al., 2015; Guo et al., 2016).
- 25 As noted, NVC concentrations may be uncertain due to low concentrations, measurement uncertainties or not measured at all. Comparing observed and predicted partitioning of NH<sub>3</sub>-NH<sub>4</sub><sup>+</sup> or HNO<sub>3</sub>-NO<sub>3</sub><sup>-</sup> provides insights on the accuracies of NVC concentrations used in the thermodynamic analysis. For example, as discussed above for the 11-13 June period in Fig. 1, the model fairly accurately predicts NH<sub>3</sub>-NH<sub>4</sub><sup>+</sup> partitioning with input of measured Na<sup>+</sup>, whereas inclusion of inferred Na<sup>+</sup> does not produce as good a result. Overall, our previously reported pH for SOAS and WINTER studies appears sufficiently accurate for
- 30 the majority of the data since the pH and predicted partitioning was in reasonable agreement with observed partitioning of NH<sub>3</sub>-NH<sub>4</sub><sup>+</sup> or HNO<sub>3</sub>-NO<sub>3</sub><sup>-</sup> without ion charge balance inferred NVC as input. (For example, see the 12-day SOAS data (Fig. 2) and the WINTER data for periods of 60-95% RH (Guo et al., 2016)). However, during periods when a bias is observed between measured and predicted partitioning, including or slightly adjusting NVC concentrations can be tested as a possible cause (note that increasing NVCs always increases the pH).
- 35 Even though the effect of NVC on pH may appear relatively small (e.g., difference of 0.2 to 0.5 pH units) the impact on predicted partitioning of a semivolatile species can be significant due to the highly non-linear response of NH<sub>3</sub>-NH<sub>4</sub><sup>+</sup> or HNO<sub>3</sub>-NO<sub>3</sub><sup>-</sup> partitioning to pH (i.e., S curve) (Guo et al., 2016; Guo et al., 2017a). For example, for SOAS average conditions, a 0.3 unit pH bias (i.e., as noted above) results in ~ 20% bias in prediction of ε(NH<sub>4</sub><sup>+</sup>) or ε(NO<sub>3</sub><sup>-</sup>) when ε(NH<sub>4</sub><sup>+</sup>) or ε(NO<sub>3</sub><sup>-</sup>) = 50%, or no bias at all when the species are completely in one phase, ε(NH<sub>4</sub><sup>+</sup>) or ε(NO<sub>3</sub><sup>-</sup>) = 0% or 100%. For the WINTER data set, a 0.5 (see
- 40 above) unit pH bias causes up to 30% bias in ε(NH<sub>4</sub><sup>+</sup>) or ε(NO<sub>3</sub><sup>-</sup>) (illustrated in Fig. S5). These partitioning biases may constitute





a significant source of bias for aerosol nitrate formation, especially if the total nitrate present in the gas-aerosol system is significant. In fact, the bias from the NVC may completely change the predicted response of nitrate to aerosol emissions and lead to errors in the predicted vs. observed trends in pH, such as was seen in the SE US (Vasilakos et al., 2017).

In our past studies, we also investigated trends in pH and molar ratios over time periods of changing emissions. Our interest was on the lack of change in pH over the past 15 years of despite a 70% reduction in sulfate aerosol (Fig. 5) (Weber et al., 2016). For example, Weber et al. (2016) reported thermodynamic calculations based on an average  $\text{PM}_{2.5}$  and  $\text{PM}_1$  PILS-IC  $\text{Na}^+$  concentration of  $0.03 \mu\text{g m}^{-3}$  from the SOAS study applied to all historical data (Fig. 2 in that paper). The  $\text{Na}^+$  concentration was uncertain due to being significantly below the  $\text{Na}^+$  measurement LOD ( $0.07 \mu\text{g m}^{-3}$ ) and substantially lower than period average  $\text{Na}^+$  of  $0.28 \mu\text{g m}^{-3}$  calculated from a charge balance. This simplification did not consider historical  $\text{Na}^+$  trends (although there was no trend in  $\text{Na}^+$  mole fraction, see Fig. 5). With a constant ISORROPIA  $\text{Na}^+$  input of  $0.03 \mu\text{g m}^{-3}$ , predicted  $R_{\text{SO}_4}$  does not follow the widespread observed trend of  $R_{\text{SO}_4}$  decreasing from 1998 to end of 2013 in the southeastern US, but instead was nearly constant at  $\sim 1.9$  (Fig. 5). Repeating the calculations using  $\text{Na}^+$  inferred from the ion charge balance of  $\text{Na}^+$ - $\text{NH}_4^+$ - $\text{SO}_4^{2-}$ - $\text{NO}_3^-$ , determined for each daily data point, results in good agreement between observed and predicted  $R_{\text{SO}_4}$ ; ISORROPIA-predicted  $R_{\text{SO}_4}$  now reproduces the observed decrease  $R_{\text{SO}_4}$  trend (Fig. 5 & Fig. S6 in the supplement). In contrast, using these different  $\text{Na}^+$  input concentrations did not change the trends in ISORROPIA-predicted pH, in both cases it remained relatively constant (Fig. S6), but as expected the pH was slightly higher with higher input  $\text{Na}^+$  concentrations (i.e., from ion charge balance).

#### 4. Summary

Excluding minor amounts of submicron NVC in thermodynamic calculations results in predicted ammonium-sulfate molar ratios ( $R$ ) near 2, which is generally higher than observed values. This results from the model criteria for aerosol electrical neutrality. Less absolute discrepancy is associated with predicted particle pH with or without NVC because pH is on a logarithmic scale of  $H_{\text{aq}}^+$  and the range of pH is larger than that of  $R$  (or  $R_{\text{SO}_4}$ ) in the eastern US. However, neglecting NVC can induce pH biases that imply important partitioning errors for semivolatile species like ammonium, nitrate, chloride, and even organic acids. An important finding is that including small amounts of NVCs in the thermodynamic model brings predicted and measured  $R$  into agreement. Because NVCs are often minor constituents of fine particles, especially for  $\text{PM}_1$ , implying low ambient concentrations and high measurement uncertainties, assessing thermodynamic model predictions through molar ratios is problematic. For the eastern US, good agreement between ISORROPIA-predicted (with measured NVCs in SOAS  $\text{PM}_{2.5}$  input and no NVC in WINTER  $\text{PM}_1$  input; no consideration of organic compounds) and measured partitioning of  $\text{NH}_3$ - $\text{NH}_4^+$  (Guo et al., 2015; Weber et al., 2016),  $\text{HNO}_3$ - $\text{NO}_3^-$  ( $> 40\%$  RH in Guo et al. (2016)) and water vapor-aerosol liquid water (Guo et al., 2015), together with a lack of correlation of the bias with organic fraction discounts any influence of organic films and validates the thermodynamic equilibrium assumption for submicron aerosol. If organic films were limiting mass transfer, the discrepancy in  $R$  should worsen as the films become thicker. We find the opposite, the discrepancy in  $R$  is positively correlated with NVC and not correlated with the organic mass fraction or mass concentration. If NVCs were not measured, or significantly below the measurement LOD, for the data sets investigated here, an ion charge balance could be used to infer NVCs. Comparing measured and thermodynamic model predicted partitioning of semivolatile species provides insights on the importance of NVCs in the model predictions. Fully considering NVC doesn't change the finding of nearly constant fine particle pH in the southeastern U.S. (summertime) despite a large sulfate reduction, the result supported by predicting a  $R_{\text{SO}_4}$  decreasing trend agreeable to the 15



years' observations. Overall, we find that the unique and non-intuitive behavior of pH reported in our past studies can be simply and consistently explained by thermodynamics without the need for organic films with selective ion transport properties.

**Acknowledgements.** This work was supported by the National Science Foundation (NSF) under grant [AGS-1360730](#). The  
5 WINTER data is provided by NCAR/EOL under sponsorship of the National Science Foundation (<http://data.eol.ucar.edu/>). AN acknowledges support from an EPA STAR grant and the European Research Council Consolidator Grant 726165 - PyroTRACH.



## References

- Allen, H. M., Draper, D. C., Ayres, B. R., Ault, A., Bondy, A., Takahama, S., Modini, R. L., Baumann, K., Edgerton, E., Knote, C., Laskin, A., Wang, B., and Fry, J. L.: Influence of crustal dust and sea spray supermicron particle concentrations and acidity on inorganic  $\text{NO}_3^-$  aerosol during the 2013 Southern Oxidant and Aerosol Study, *Atm. Chem. Phys.*, 15, 10669-10685, doi: 10.5194/acp-15-10669-2015, 2015.
- Attwood, A. R., Washenfelder, R. A., Brock, C. A., Hu, W., Baumann, K., Campuzano-Jost, P., Day, D. A., Edgerton, E. S., Murphy, D. M., Palm, B. B., McComiskey, A., Wagner, N. L., de Sa, S. S., Ortega, A., Martin, S. T., Jimenez, J. L., and Brown, S. S.: Trends in sulfate and organic aerosol mass in the Southeast U.S.: Impact on aerosol optical depth and radiative forcing, *Geophysical Research Letters*, 41, 7701-7709, doi: 10.1002/2014gl061669, 2014.
- 10 Bahreini, R., Ervens, B., Middlebrook, A. M., Warneke, C., de Gouw, J. A., DeCarlo, P. F., Jimenez, J. L., Brock, C. A., Neuman, J. A., Ryerson, T. B., Stark, H., Atlas, E., Brioude, J., Fried, A., Holloway, J. S., Peischl, J., Richter, D., Walega, J., Weibring, P., Wollny, A. G., and Fehsenfeld, F. C.: Organic aerosol formation in urban and industrial plumes near Houston and Dallas, Texas, *Journal of Geophysical Research*, 114, D00F16, doi: 10.1029/2008jd011493, 2009.
- 15 Blanchard, C. L., Hidy, G. M., Tanenbaum, S., Edgerton, E. S., and Hartsell, B. E.: The Southeastern Aerosol Research and Characterization (SEARCH) study: Spatial variations and chemical climatology, 1999–2010, *Journal of the Air & Waste Management Association*, 63, 260-275, doi: 10.1080/10962247.2012.749816, 2013.
- Bones, D. L., Reid, J. P., Lienhard, D. M., and Krieger, U. K.: Comparing the mechanism of water condensation and evaporation in glassy aerosol, *Proc Natl Acad Sci USA*, 109, 11613-11618, doi: 10.1073/pnas.1200691109, 2012.
- 20 Bougiatioti, A., Nikolaou, P., Stavroulas, I., Kouvarakis, G., Weber, R., Nenes, A., Kanakidou, M., and Mihalopoulos, N.: Particle water and pH in the Eastern Mediterranean: Sources variability and implications for nutrients availability, *Atm. Chem. Phys.*, 16, 4579-4591, doi: 10.5194/acp-16-4579-2016, 2016.
- Cruz, C. N., Dassios, K. G., and Pandis, S. N.: The effect of dioctyl phthalate films on the ammonium nitrate aerosol evaporation rate, *Atmospheric Environment*, 34, 3897-3905, doi: 10.1016/S1352-2310(00)00173-4, 2000.
- 25 Dassios, K. G., and Pandis, S. N.: The mass accommodation coefficient of ammonium nitrate aerosol, *Atmospheric Environment*, 33, 2993-3003, doi: 10.1016/S1352-2310(99)00079-5, 1999.
- DeCarlo, P. F., Kimmel, J. R., Trimborn, A., Northway, M. J., Jayne, J. T., Aiken, A. C., Gonin, M., Fuhrer, K., Horvath, T., Docherty, K. S., Worsnop, D. R., and Jimenez, J. L.: Field-deployable, high-resolution, time-of-flight aerosol mass spectrometer, *Anal Chem*, 78, 8281-8289, doi: 10.1021/ac061249n, 2006.
- 30 Eddingsaas, N. C., VanderVelde, D. G., and Wennberg, P. O.: Kinetics and Products of the Acid-Catalyzed Ring-Opening of Atmospherically Relevant Butyl Epoxy Alcohols, *J Phys Chem A*, 114, 8106-8113, doi: 10.1021/Jp103907c, 2010.
- Fang, T., Guo, H., Zeng, L., Verma, V., Nenes, A., and Weber, R. J.: Highly Acidic Ambient Particles, Soluble Metals, and Oxidative Potential: A Link between Sulfate and Aerosol Toxicity, *Environ Sci Technol*, 51, 2611-2620, doi: 10.1021/acs.est.6b06151, 2017.
- 35 Fountoukis, C., and Nenes, A.: ISORROPIA II: a computationally efficient thermodynamic equilibrium model for  $\text{K}^+$ - $\text{Ca}^{2+}$ - $\text{Mg}^{2+}$ - $\text{NH}_4^+$ - $\text{Na}^+$ - $\text{SO}_4^{2-}$ - $\text{NO}_3^-$ - $\text{Cl}^-$ - $\text{H}_2\text{O}$  aerosols, *Atm. Chem. Phys.*, 7, 4639-4659, doi: 10.5194/acp-7-4639-2007, 2007.
- Fountoukis, C., Nenes, A., Sullivan, A., Weber, R., Van Reken, T., Fischer, M., Matias, E., Moya, M., Farmer, D., and Cohen, R. C.: Thermodynamic characterization of Mexico City aerosol during MILAGRO 2006, *Atm. Chem. Phys.*, 9, 2141-2156, doi: 10.5194/acp-9-2141-2009, 2009.
- 40 Guo, H., Xu, L., Bougiatioti, A., Cerully, K. M., Capps, S. L., Hite, J. R., Carlton, A. G., Lee, S. H., Bergin, M. H., Ng, N. L., Nenes, A., and Weber, R. J.: Fine-particle water and pH in the southeastern United States, *Atm. Chem. Phys.*, 15, 5211-5228, doi: 10.5194/acp-15-5211-2015, 2015.
- 45 Guo, H., Sullivan, A. P., Campuzano-Jost, P., Schroder, J. C., Lopez-Hilfiker, F. D., Dibb, J. E., Jimenez, J. L., Thornton, J. A., Brown, S. S., Nenes, A., and Weber, R. J.: Fine particle pH and the partitioning of nitric acid during winter in the northeastern United States, *Journal of Geophysical Research: Atmospheres*, 121, 10355-10376, doi: 10.1002/2016jd025311, 2016.
- Guo, H., Liu, J., Froyd, K. D., Roberts, J. M., Veres, P. R., Hayes, P. L., Jimenez, J. L., Nenes, A., and Weber, R. J.: 50 Fine particle pH and gas-particle phase partitioning of inorganic species in Pasadena, California, during the 2010 CalNex campaign, *Atm. Chem. Phys.*, 17, 5703-5719, doi: 10.5194/acp-17-5703-2017, 2017a.
- Guo, H., Weber, R., and Nenes, A.: The sensitivity of particle pH to  $\text{NH}_3$ : Can high  $\text{NH}_3$  cause London Fog conditions?, In review, 2017b.



- Hand, J. L., Schichtel, B. A., Malm, W. C., and Pitchford, M. L.: Particulate sulfate ion concentration and SO<sub>2</sub> emission trends in the United States from the early 1990s through 2010, *Atm. Chem. Phys.*, 12, 10353-10365, doi: 10.5194/acp-12-10353-2012, 2012.
- 5 Hennigan, C. J., Izumi, J., Sullivan, A. P., Weber, R. J., and Nenes, A.: A critical evaluation of proxy methods used to estimate the acidity of atmospheric particles, *Atm. Chem. Phys.*, 15, 2775-2790, doi: 10.5194/acp-15-2775-2015, 2015.
- Hidy, G. M., Blanchard, C. L., Baumann, K., Edgerton, E., Tanenbaum, S., Shaw, S., Knipping, E., Tombach, I., Jansen, J., and Walters, J.: Chemical climatology of the southeastern United States, 1999-2013, *Atm. Chem. Phys.*, 14, 11893-11914, doi: 10.5194/acp-14-11893-2014, 2014.
- 10 Jang, M., Czoschke, N. M., Lee, S., and Kamens, R. M.: Heterogeneous atmospheric aerosol production by acid-catalyzed particle-phase reactions, *Science*, 298, 814-817, doi: 10.1126/science.1075798, 2002.
- Keene, W. C., Sander, R., Pszenny, A. A. P., Vogt, R., Crutzen, P. J., and Galloway, J. N.: Aerosol pH in the marine boundary layer: A review and model evaluation, *Journal of Aerosol Science*, 29, 339-356, doi: 10.1016/s0021-8502(97)10011-8, 1998.
- 15 Kim, P. S., Jacob, D. J., Fisher, J. A., Travis, K., Yu, K., Zhu, L., Yantosca, R. M., Sulprizio, M. P., Jimenez, J. L., Campuzano-Jost, P., Froyd, K. D., Liao, J., Hair, J. W., Fenn, M. A., Butler, C. F., Wagner, N. L., Gordon, T. D., Welti, A., Wennberg, P. O., Crouse, J. D., St Clair, J. M., Teng, A. P., Millet, D. B., Schwarz, J. P., Markovic, M. Z., and Perring, A. E.: Sources, seasonality, and trends of southeast US aerosol: an integrated analysis of surface, aircraft, and satellite observations with the GEOS-Chem chemical transport model, *Atm. Chem. Phys.*, 15, 10411-20 10433, doi: 10.5194/acp-15-10411-2015, 2015.
- Longo, A. F., Feng, Y., Lai, B., Landing, W. M., Shelley, R. U., Nenes, A., Mihalopoulos, N., Violaki, K., and Ingall, E. D.: Influence of Atmospheric Processes on the Solubility and Composition of Iron in Saharan Dust, *Environ Sci Technol*, 50, 6912-6920, doi: 10.1021/acs.est.6b02605, 2016.
- Meskhidze, N., Chameides, W. L., Nenes, A., and Chen, G.: Iron mobilization in mineral dust: Can anthropogenic 25 SO<sub>2</sub> emissions affect ocean productivity?, *Geophysical Research Letters*, 30, 2085, doi: 10.1029/2003gl018035, 2003.
- Nenes, A., Krom, M. D., Mihalopoulos, N., Van Cappellen, P., Shi, Z., Bougiatioti, A., Zampas, P., and Herut, B.: Atmospheric acidification of mineral aerosols: a source of bioavailable phosphorus for the oceans, *Atm. Chem. Phys.*, 11, 6265-6272, doi: 10.5194/acp-11-6265-2011, 2011.
- 30 Orsini, D. A., Ma, Y., Sullivan, A., Sierau, B., Baumann, K., and Weber, R. J.: Refinements to the particle-into-liquid sampler (PILS) for ground and airborne measurements of water soluble aerosol composition, *Atmospheric Environment*, 37, 1243-1259, doi: 10.1016/s1352-2310(02)01015-4, 2003.
- Paulot, F., and Jacob, D. J.: Hidden cost of U.S. agricultural exports: particulate matter from ammonia emissions, *Environ Sci Technol*, 48, 903-908, doi: 10.1021/es4034793, 2014.
- 35 Rindelaub, J. D., Craig, R. L., Nandy, L., Bondy, A. L., Dutcher, C. S., Shepson, P. B., and Ault, A. P.: Direct Measurement of pH in Individual Particles via Raman Microspectroscopy and Variation in Acidity with Relative Humidity, *J Phys Chem A*, 120, 911-917, doi: 10.1021/acs.jpca.5b12699, 2016.
- Silvern, R. F., Jacob, D. J., Kim, P. S., Marais, E. A., Turner, J. R., Campuzano-Jost, P., and Jimenez, J. L.: Inconsistency of ammonium-sulfate aerosol ratios with thermodynamic models in the eastern US: a possible role of 40 organic aerosol, *Atm. Chem. Phys.*, 17, 5107-5118, doi: 10.5194/acp-17-5107-2017, 2017.
- Surratt, J. D., Chan, A. W., Eddingsaas, N. C., Chan, M., Loza, C. L., Kwan, A. J., Hersey, S. P., Flagan, R. C., Wennberg, P. O., and Seinfeld, J. H.: Reactive intermediates revealed in secondary organic aerosol formation from isoprene, *Proc Natl Acad Sci USA*, 107, 6640-6645, doi: 10.1073/pnas.0911114107, 2010.
- Tong, H. J., Reid, J. P., Bones, D. L., Luo, B. P., and Krieger, U. K.: Measurements of the timescales for the mass 45 transfer of water in glassy aerosol at low relative humidity and ambient temperature, *Atm. Chem. Phys.*, 11, 4739-4754, doi: 10.5194/acp-11-4739-2011, 2011.
- Vasilakos, P., Russell, A. G., Weber, R. J., and Nenes, A.: Understanding nitrate formation in a world with less sulfate, In review, 2017.
- Wang, G., Zhang, R., Gomez, M. E., Yang, L., Levy Zamora, M., Hu, M., Lin, Y., Peng, J., Guo, S., Meng, J., Li, J., 50 Cheng, C., Hu, T., Ren, Y., Wang, Y., Gao, J., Cao, J., An, Z., Zhou, W., Li, G., Wang, J., Tian, P., Marrero-Ortiz, W., Secret, J., Du, Z., Zheng, J., Shang, D., Zeng, L., Shao, M., Wang, W., Huang, Y., Wang, Y., Zhu, Y., Li, Y., Hu, J., Pan, B., Cai, L., Cheng, Y., Ji, Y., Zhang, F., Rosenfeld, D., Liss, P. S., Duce, R. A., Kolb, C. E., and Molina, M. J.: Persistent sulfate formation from London Fog to Chinese haze, *Proc Natl Acad Sci USA*, 113, 13630-13635, doi: 10.1073/pnas.1616540113, 2016.



- Weber, R. J., Guo, H., Russell, A. G., and Nenes, A.: High aerosol acidity despite declining atmospheric sulfate concentrations over the past 15 years, *Nature Geoscience*, 9, 282-285, doi: 10.1038/ngeo2665, 2016.
- You, Y., Kanawade, V. P., de Gouw, J. A., Guenther, A. B., Madronich, S., Sierra-Hernandez, M. R., Lawler, M., Smith, J. N., Takahama, S., Ruggeri, G., Koss, A., Olson, K., Baumann, K., Weber, R. J., Nenes, A., Guo, H.,  
5 Edgerton, E. S., Porcelli, L., Brune, W. H., Goldstein, A. H., and Lee, S. H.: Atmospheric amines and ammonia measured with a chemical ionization mass spectrometer (CIMS), *Atm. Chem. Phys.*, 14, 12181-12194, doi: 10.5194/acp-14-12181-2014, 2014.
- Zhang, Q., Jimenez, J. L., Canagaratna, M. R., Allan, J. D., Coe, H., Ulbrich, I., Alfarra, M. R., Takami, A., Middlebrook, A. M., Sun, Y. L., Dzepina, K., Dunlea, E., Docherty, K., DeCarlo, P. F., Salcedo, D., Onasch, T.,  
10 Jayne, J. T., Miyoshi, T., Shimo, A., Hatakeyama, S., Takegawa, N., Kondo, Y., Schneider, J., Drewnick, F., Borrmann, S., Weimer, S., Demerjian, K., Williams, P., Bower, K., Bahreini, R., Cottrell, L., Griffin, R. J., Rautiainen, J., Sun, J. Y., Zhang, Y. M., and Worsnop, D. R.: Ubiquity and dominance of oxygenated species in organic aerosols in anthropogenically-influenced Northern Hemisphere midlatitudes, *Geophysical Research Letters*, 34, L13801, doi: 10.1029/2007gl029979, 2007.
- 15 Zhuang, H., Chan, C. K., Fang, M., and Wexler, A. S.: Size distributions of particulate sulfate, nitrate, and ammonium at a coastal site in Hong Kong, *Atmospheric Environment*, 33, 843-853, doi: 10.1016/S1352-2310(98)00305-7, 1999.

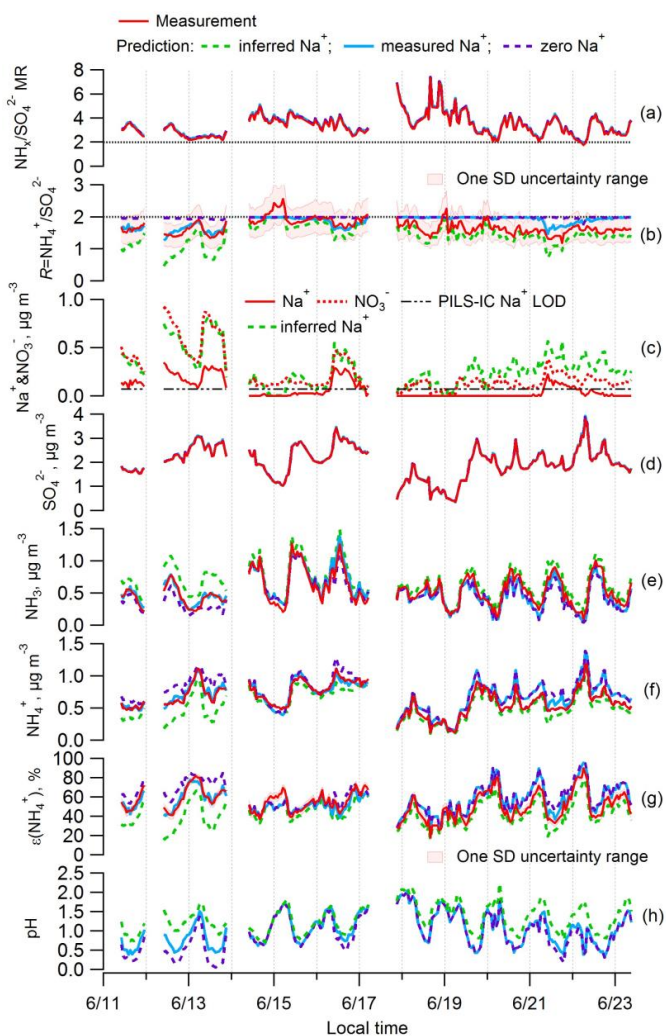
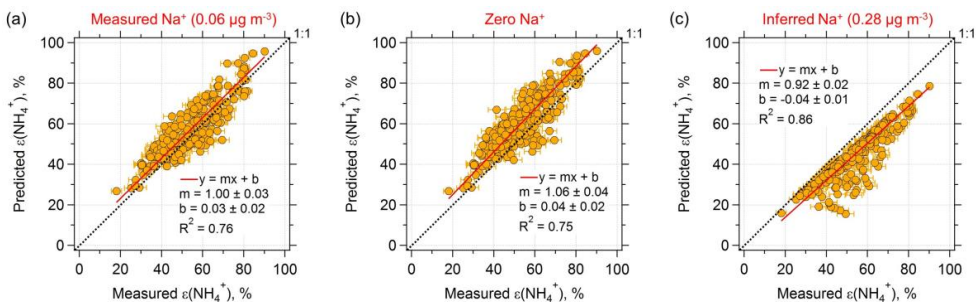


Figure 1. Time series of various measured and ISORROPIA-predicted parameters and  $\text{PM}_{2.5}$  component concentrations for a select period of the SOAS study, with periods of rainfall removed. Three ISORROPIA-predicted results are shown at different  $\text{Na}^+$  levels; calculated  $\text{Na}^+$  needed for ion charge balance ( $\text{Na}^+ = 2\text{SO}_4^{2-} + \text{NO}_3^- + \text{Cl}^- - \text{NH}_4^+$ ,  $\mu\text{mol m}^{-3}$ ; mean value of  $0.28 \pm 0.18 \mu\text{g m}^{-3}$ ) in green, measured  $\text{Na}^+$  blue, and zero  $\text{Na}^+$  in purple. All other inputs were the same.  $\text{Na}^+$  represents generic non-volatile cations (NVC). Specific plots are as follows: (a) total ammonium ( $\text{NH}_x = \text{NH}_4^+ + \text{NH}_3$ ) to sulfate molar ratio ( $(\text{NH}_x/\text{SO}_4^{2-})_{\text{MIR}}$ ), (b) aerosol ammonium-sulfate ratios ( $R = \text{NH}_4^+/\text{SO}_4^{2-}$ ), (c)  $\text{Na}^+$  and  $\text{NO}_3^-$ , (d)  $\text{SO}_4^{2-}$ , (e)  $\text{NH}_3$ , (f)  $\text{NH}_4^+$ , (g) particle-phase fractions of total ammonium,  $\epsilon(\text{NH}_4^+)$ , and (h) particle pH.





**Figure 2.** Comparisons of predicted and measured particle phase fractions of total ammonium,  $\varepsilon(\text{NH}_4^+) = \text{NH}_4^+ / (\text{NH}_3 + \text{NH}_4^+)$ , for a 12-day period data from the SOAS study.  $\text{NH}_4^+$  was measured with a PILS-IC ( $\text{PM}_{2.5}$  cut size) and  $\text{NH}_3$  from a CIMS. (a) The model prediction is based on an ISORROPIA input of measured  $\text{Na}^+$ ,  $(\text{NH}_4^+ + \text{NH}_3)$ ,  $\text{SO}_4^{2-}$ ,  $\text{NO}_3^-$ ,  $\text{Cl}^-$ ; (b) Model input is identical to (a), except that  $\text{Na}^+$  is set to zero; (c) Same model input, but  $\text{Na}^+$  is inferred from an ion charge balance. Orthogonal distance regression (ODR) fits are shown and uncertainties in the fits are one standard deviation (SD). Uncertainty of measured  $\varepsilon(\text{NH}_4^+)$  is derived from error propagation of  $\text{NH}_4^+$  (20%) and  $\text{NH}_3$  (6.8%) measurements. Best agreement is achieved by using measured  $\text{Na}^+$  as input. In general, very good prediction of  $\text{NH}_3$ - $\text{NH}_4^+$  partitioning was achieved by a thermodynamic model without including organic species.

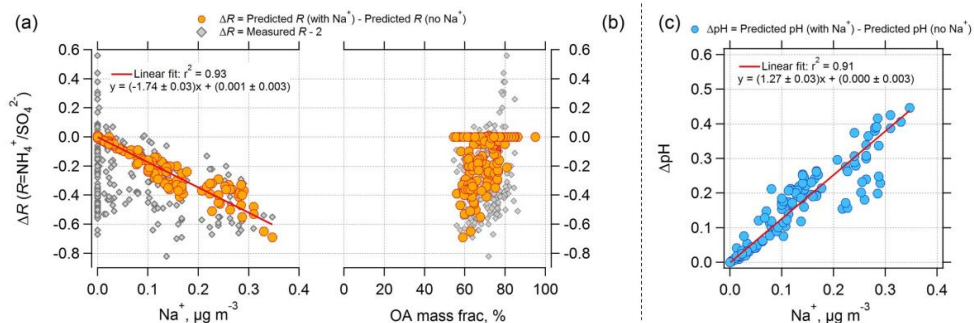


Figure 3. Effect of nonvolatile cations (NVC) on the  $\text{PM}_{2.5}$  ammonium-sulfate molar ratio ( $R$ ) and pH as a function of measured  $\text{Na}^+$  concentration and organic aerosol (OA) mass fractions. The orange circular points in plots (a) and (b) are for  $\Delta R$  equal to ISORROPIA predicted  $R$  with measured  $\text{Na}^+$  included in the model input minus ISORROPIA predicted  $R$  without  $\text{Na}^+$  in the model input.  $\Delta \text{pH}$  in plot (c) is determined in a similar way. The grey diamonds in plots (a) and (b) are for  $\Delta R$  equal to the actual measured  $R$  minus 2. Note that  $\Delta R$  should be negative since including  $\text{Na}^+$  in the thermodynamic model results in  $R$  lower than 2, whereas not including  $\text{Na}^+$  results in an  $R$  close to 2 (on average  $R$  predicted without  $\text{Na}^+$  is  $1.97 \pm 0.02$ ), a measured  $R$  is generally less than 2. Plot (a) is  $\Delta R$  versus measured  $\text{Na}^+$ , (b)  $\Delta R$  versus measured OA mass fraction, and (c)  $\Delta \text{pH}$  versus measured  $\text{Na}^+$ . Orthogonal distance regression (ODR) fits are shown and uncertainties in the fits are one standard deviation. A plot similar to (b), but versus OA mass concentration can be found as Fig. S2 in the supplemental material.

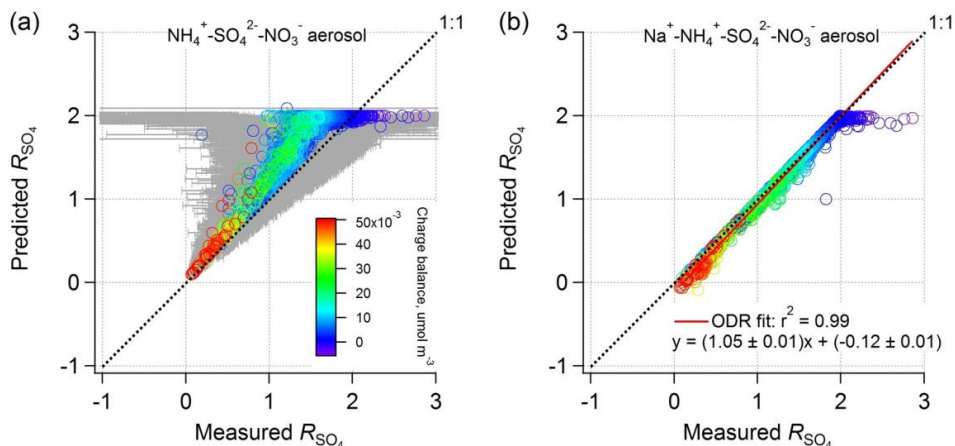
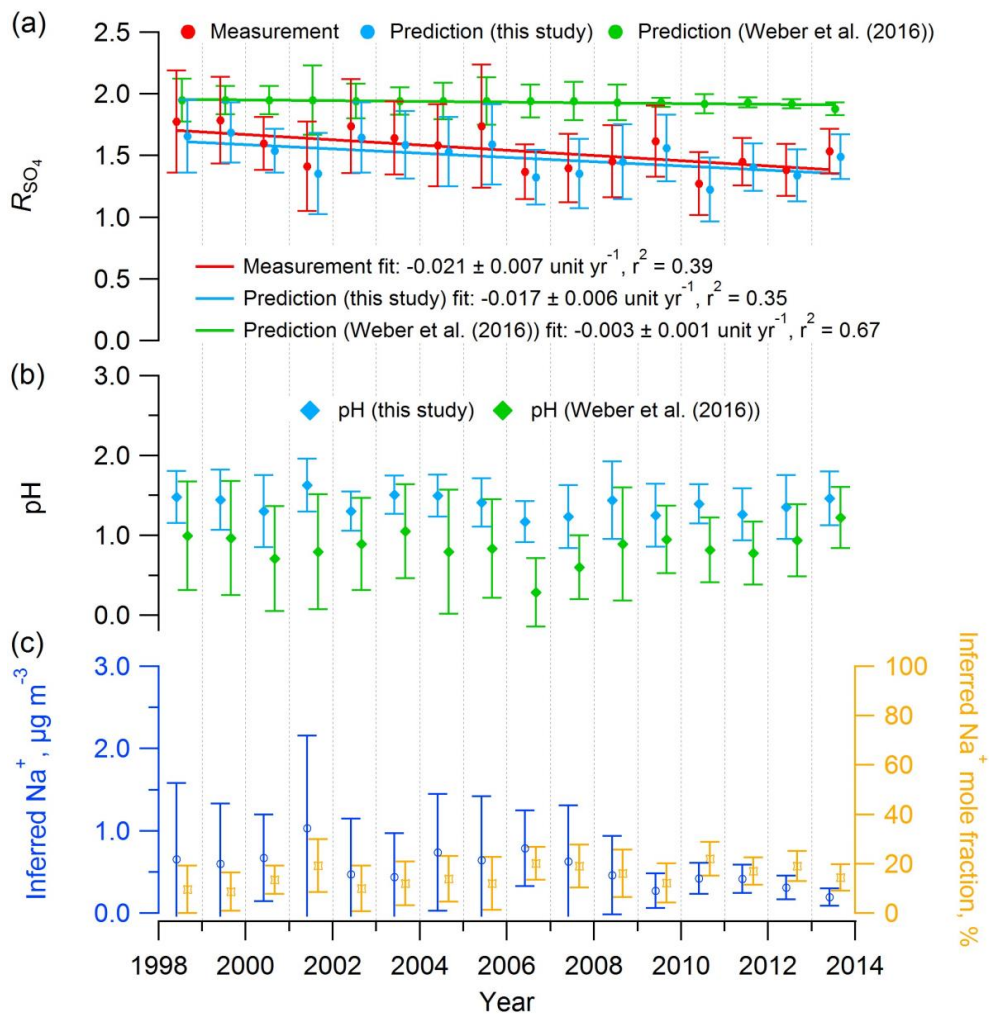


Figure 4. Comparison between PM<sub>1</sub> ISORROPIA-predicted  $R_{\text{SO}_4}$  and AMS-measured  $R_{\text{SO}_4}$  ( $R_{\text{SO}_4} = (\text{NH}_4^+ - \text{NO}_3^-)/\text{SO}_4^{2-}$ ) (mol mol<sup>-1</sup>), where the ISORROPIA-prediction is based on (a)  $\text{NH}_4^+ - \text{SO}_4^{2-} - \text{NO}_3^-$  aerosol and (b)  $\text{Na}^+ - \text{NH}_4^+ - \text{SO}_4^{2-} - \text{NO}_3^-$  aerosol both constrained by  $\text{HNO}_3$ . All measurement data are from the WINTER study. NVC was determined by an ion charge balance with the molar concentration shown as the color wave. For this data, the average predicted  $\text{Na}^+$  concentration is  $0.15 \mu\text{g m}^{-3}$ , comparable to the offline PILS fraction collector IC-measured PM<sub>1</sub>  $\text{Na}^+$  of  $0.23 \mu\text{g m}^{-3}$ . The one SD uncertainty range for the measured  $R_{\text{SO}_4}$  is shown as gray error bars. The data points with low  $\text{SO}_4^{2-}$  levels ( $<0.2 \mu\text{g m}^{-3}$ ; 9% of the total points) were excluded for high uncertainties. In both plots, the molar ratios are zero when concentrations of  $\text{NH}_4^+$  are near zero and NVC concentrations highest. In plot (a), as molar ratios approach 2, predicted NVC levels drop, but the effect of not including them in the thermodynamic model results in larger deviations in predicted versus measured  $R_{\text{SO}_4}$ . Error bars also increase due to subtraction of higher concentrations of nitrate and thus more subject to measurement error. As with the SOAS data, including NVC in the model results in agreement between predicted and measured ammonium-sulfate molar ratios.





**Figure 5.** Mean summer (June–August) trends in (a) measured and predicted  $R_{\text{SO}_4}$ , (b) predicted  $\text{PM}_{2.5}$  pH, and (c) inferred  $\text{Na}^+$  (from ion charge balance of  $\text{Na}^+$ - $\text{NH}_4^+$ - $\text{SO}_4^{2-}$ - $\text{NO}_3^-$  aerosols) concentration and mole fraction at the SEARCH-CTR site. Model input includes the observational  $\text{PM}_{2.5}$  composition data ( $\text{NH}_4^+$ ,  $\text{SO}_4^{2-}$ ,  $\text{NO}_3^-$ ) and meteorological data (RH, T) at CTR.  $R_{\text{SO}_4}$  and pH were estimated with ISORROPIA-II run in forward mode with an assumed  $\text{NH}_3$  level of  $0.36 \mu\text{g m}^{-3}$ , the mean concentration from the SOAS study (CTR site, summer 2013), due to limited  $\text{NH}_3$  data before 2008. Historical  $\text{NH}_3$  mean summer concentration at CTR were  $0.2 \mu\text{g m}^{-3}$  (2004–2007) (Blanchard et al., 2013) and  $0.23 \pm 0.14 \mu\text{g m}^{-3}$  (2008–2013) (Weber et al., 2016). 41 out of the total 609 (7%) daily mean  $R_{\text{SO}_4}$  were observed above 3 due to measurement error, above the upper limit of  $R_{\text{SO}_4} = 2$ , therefore, excluded in the model input. Error bars represent daily data ranges (SD). Linear regression fits are shown and uncertainties in the fits are one SD. In (a), based on regression slope, the observed  $R_{\text{SO}_4}$  trend was  $-0.021 \pm 0.007$  at CTR versus a predicted value of  $-0.017 \pm 0.006 \text{ unit yr}^{-1}$  for ISORROPIA run with  $\text{Na}^+$  from the charge balance, and  $-0.003 \pm 0.001 \text{ unit yr}^{-1}$  for a constant  $\text{Na}^+$  of  $0.03 \mu\text{g m}^{-3}$ , used by Weber et al. (2016). These results are consistent with the reported  $R_{\text{SO}_4}$  trend of  $-0.01$  to  $-0.03 \text{ yr}^{-1}$  reported by Hidy et al. (2014) for SEARCH data set. In (b), the pH predictions with inferred  $\text{Na}^+$  or with limited  $\text{Na}^+$  of  $0.03 \mu\text{g m}^{-3}$  shows a fairly stable  $\text{PM}_{2.5}$  pH in the last 15 years. In (c), the inferred  $\text{Na}^+$  shows a general decreasing trend while the inferred  $\text{Na}^+$  mole fraction stays relatively stable around 15% ( $\pm 4\%$ ).